Computational Modelling of SOL and Divertor Plasmas at JET

A Taroni, G Corrigan, G J Radford, R Simonini,
J Spence, S A Weber.

JET Joint Undertaking, Abingdon, Oxfordshire, OX14 3EA, UK.

ABSTRACT

The code EDGE2D/U developed at JET to simulate the external region of Tokamak plasmas is described, discussing the related physical, mathematical and numerical problems. Results of a numerical study of the problem of plasma detachment in JET are presented.

Introduction

Two dimensional (2D) multi-fluid transport codes to simulate the complex phenomena taking place in the external plasma region of a tokamak where the magnetic field lines are open and intersect material walls have become important tools for the interpretation of measurements of plasma quantitites in the boundary region. They are also used to provide indications on the possible performance of divertors being designed, both for existing and for proposed devices and in particular ITER. For recent review papers on existing codes see [1], [2].

JET has a large divertor physics programme and computational modelling of SOL and divertor plasmas plays an important role in this programme. To satisfy the needs of this programme a chain of codes properly interconnected [3] has been developed, whose main elements are EDGE2D/U, solving the 2D particle, momentum and energy conservation equations for a multi-fluid plasma, and NIMBUS a Monte Carlo code dealing with neutral species [4].

In the first part of this paper we present the main features of EDGE2D/U, discussing the equations solved and the boundary conditions implemented to determine a solution. These conditions are fully compatible with the mathematical nature of the problem, and simulate as closely as possible the external constraints and experimental 'knobs' determining the plasma evolution in the outer plasma region. We also give a brief survey of the numerical methods used to solve the equations on a non uniform and non orthogonal finite difference mesh. Indeed physical, mathematical, and numerical problems are strictly correlated and have to be dealt with in parallel in this field of plasma physics.

In the second part of the paper we present the results of a numerical study of the conditions required to obtain plasma detachment in a gas box divertor configuration being designed for JET, showing the close correlation between the problem of power exhaust and impurity control in an ITER relevant divertor.

Equations and Conditions Determining a Solution

The equations

Fluid equations for the conservation of particles, momentum, and energy, are solved in EDGE2D/U for hydrogenic and impurity ions over a region that extends beyond the separatrix as far as material obstacles allow, and a few centimetres inside the separatrix. The model allows for an arbitrarily high concentration of an impurity species. The full non-coronal distribution of the impurity charge states is determined consistently together with the corresponding power loss terms, using cross sections from the ADAS data base for the atomic processes for the different ionisation stages [5].
Assuming toroidal symmetry the equations to be solved can be written in an orthogonal system of coordinates in the poloidal plane with metric given by:

$$ds^2 = H_\rho^2 d\rho^2 + H_\theta^2\, d\theta^2 + R^2 d\phi^2$$

with ρ labelling the magnetic flux surfaces and θ being a coordinate in the poloidal direction orthogonal to ρ.
Neglecting drift terms within the magnetic flux surfaces, representing vector and tensor quantities by their components parallel to magnetic field lines and perpendicular to magnetic surfaces, and using standard notation when not specified, the equations are as follows:

Density equation for each species (α = i, hydrogenic ions, α = z impurity ions of charge z):

$$\frac{\partial n_\alpha}{\partial t} + \frac{1}{H}\frac{\partial}{\partial \rho}\left(\frac{H}{H_\rho} n_\alpha v_{\alpha,\rho}\right) + \frac{1}{H}\frac{\partial}{\partial \theta}\left(\frac{H h_\theta}{H_\theta} n_\alpha v_\alpha\right) = S_\alpha \qquad (1)$$

where $h_\theta = \frac{B_\theta}{B}, h_\phi = \frac{B_\phi}{B}, v_\alpha$ represents the parallel component of the velocity and the perpendicular components are usually modelled as:

$$v_{i,\rho} = \frac{-D}{n_i H_\rho}\frac{\partial n_i}{\partial \rho} - C_{th}\frac{cB_\phi}{eB^2 H_\theta}\frac{\partial T_e}{\partial \theta} \quad \text{and} \quad v_{z,\rho} = \frac{-D_z}{n_z H_\rho}\frac{\partial n_z}{\partial \rho}$$

Parallel momentum equation for each species:

$$\frac{\partial}{\partial t}(m_\alpha n_\alpha v_\alpha)+\frac{1}{H}\frac{\partial}{\partial_\rho}\left(\frac{H}{H_\rho}m_\alpha n_\alpha v_{\alpha,\rho}v_\alpha\right)+\frac{1}{H}\frac{\partial}{\partial\theta}\left(\frac{Hh_\theta}{H_\theta}m_\alpha n_\alpha {v_\alpha}^2\right)= \tag{2}$$

$$=-\frac{h_\theta}{H_\theta}\frac{\partial p_\alpha}{\partial\theta}+\Pi_{\alpha,\|}+\Pi_{\alpha,\rho}+Z_\alpha e n_\alpha E+R_{\alpha e}+\sum_{\alpha'\neq\alpha}R_{\alpha\alpha'}+F_\alpha$$

where:

$$\Pi_{\alpha,\|}=\frac{1}{H}\frac{\partial}{\partial\theta}\left(\frac{4}{3}\eta_{o,\alpha}\frac{{h_\theta}^2 H}{{H_\theta}^2}\frac{\partial v_\alpha}{\partial\theta}\right)\qquad \Pi_{\alpha,\rho}=\frac{1}{H}\frac{\partial}{\partial\rho}\left(\eta_{\rho,\alpha}\frac{H}{{H_\rho}^2}\frac{\partial v_\alpha}{\partial\rho}\right)$$

$$\eta_{\rho,\alpha}\propto m_\alpha D_\alpha\quad,\quad E=\eta j_\| -\frac{h_\theta}{H_\theta}\left(\frac{1}{en_e}\frac{\partial p_e}{\partial\theta}+\frac{C_{th}}{e}\frac{\partial T_e}{\partial\theta}\right)$$

Here $\eta_{\rho,\alpha}$ and $\eta_{o,\alpha}$ are viscosity coefficients, while η is the parallel resistivity.

Electron temperature equation:

$$\frac{3}{2}\frac{\partial p_e}{\partial t}+\frac{1}{H}\frac{\partial}{\partial\rho}\left[\frac{H}{H_\rho}\left(\frac{5}{2}p_e v_{e,\rho}+\frac{5}{2}n_e\frac{cT_e B_\phi}{eB^2H_\theta}\frac{\partial T_e}{\partial\theta}-k_{e,\rho}\frac{1}{H_\rho}\frac{\partial T_e}{\partial\rho}\right)\right]+$$

$$+\frac{1}{H}\frac{\partial}{\partial\theta}\left[\frac{Hh_\theta}{H_\theta}\left(\frac{5}{2}p_e v_e-k_e\frac{h_\theta}{H_\theta}\frac{\partial T_e}{\partial\theta}\right)\right]=v_{e,\rho}\frac{1}{H_\rho}\frac{\partial p_e}{\partial\rho}+v_e\frac{h_\theta}{H_\theta}\frac{\partial p_e}{\partial\theta}+ \tag{3}$$

$$+\eta {j_\|}^2-\frac{j_\|}{e}C_{th}\frac{h_\theta}{H_\theta}\frac{\partial T_e}{\partial\theta}-\sum_\alpha Q_{e\alpha}+Q_e$$

where;

$$Q_{e\alpha}=3\frac{m_e}{\tau_e}\frac{n_\alpha {Z_\alpha}^2}{m_\alpha}(T_e-T_i)\quad,\quad v_e=\frac{1}{n_e}\left(n_i v_i+\sum_z n_z Z v_z-\frac{j_\|}{e}\right)$$

$$v_{e,\rho}=\frac{-D}{n_e H_\rho}\frac{\partial n_i}{\partial\rho}-C_{th}\frac{cB_\phi}{eB^2H_\theta}\frac{\partial T_e}{\partial\theta}$$

Ion temperature equation:

$$\frac{3}{2}\frac{\partial\sum p_\alpha}{\partial t}+\frac{1}{H}\frac{\partial}{\partial\rho}\left[\frac{H}{H_\rho}\left(\frac{5}{2}\sum p_\alpha v_{\alpha,\rho}-\frac{5}{2}n_i\frac{cT_iB_\phi}{eB^2H_\theta}\frac{\partial T_i}{\partial\theta}-k_{i,\rho}\frac{1}{H_\rho}\frac{\partial T_i}{\partial\rho}\right)\right]+$$

$$+\frac{1}{H}\frac{\partial}{\partial\theta}\left[\frac{Hh_\theta}{H_\theta}\left(\frac{5}{2}\sum p_\alpha v_\alpha-k_i\frac{h_\theta}{H_\theta}\frac{\partial T_i}{\partial\theta}\right)\right]=\sum_\alpha v_{\alpha,\rho}\frac{1}{H_\rho}\frac{\partial p_\alpha}{\partial\rho}+\sum_\alpha v_\alpha\frac{h_\theta}{H_\theta}\frac{\partial p_\alpha}{\partial\theta}+ \qquad (4)$$

$$+\sum_\alpha Q_{e\alpha}+Q_i$$

The parallel current $j_{||}$ is computed from Ohm's law assuming $j_{||} >> j_\perp$, which yields [6]:

$$j_{||}=\frac{H_\theta}{Hh_\theta}\frac{1}{\int_{\theta_1}^{\theta_2}\frac{H_\theta^2}{Hh_\theta^2}\eta_{||}d\theta}\left[\int_{\theta_1}^{\theta_2}\frac{1}{en}\frac{\partial p_e}{\partial\theta}d\theta+\phi_1-\phi_2+\int_{\theta_1}^{\theta_2}\frac{C_{th}}{e}\frac{\partial T_e}{\partial\theta}d\theta\right]$$

where the potential drops ϕ_1 and ϕ_2 at the targets 1 and 2 are determined according to sheath theory from:

$$\left[j_{||}\right]_{1,2}=e\left[n_iv_i+\sum n_zZv_z-n_e\frac{v_e}{2\sqrt{\pi}}e^{-e\phi/T_e}\right]_{1,2}$$

The collisional parallel transport coefficients k_e, k_i, $\eta_{0,\alpha}$, the interspecies friction and thermoelectric forces $R_{\alpha e}$, $R_{\alpha\alpha}$, and the coefficient C_{th} are given in [6-8] . Detailed expressions for the volume source terms can be found elsewhere [4], [5], [9]. These terms require profiles of density and temperature of neutrals that are computed by the Monte Carlo Code NIMBUS.

Both first order and second order space derivatives appear in the equations showing the mixed hyperbolic-parabolic nature of the system. This is typical of non ideal, time dependent fluid dynamics equations.

The system differs from standard fluid dynamics equations because a purely diffusive particle flow is assumed in perpendicular direction. Thus the system is dominated by diffusion in this direction while convection dominates the flow in parallel direction and competes with diffusion for energy transport.

We recall from mathematical and numerical analysis that in the case of a purely convective equation a boundary condition can be prescribed only if the flow points away from the boundary. If the hyperbolic character is only slightly perturbed by a dissipative second derivative term, a mild condition such as an extrapolated value for the unknown can be

imposed safely. Stronger conditions are likely to introduce numerical inaccuracy. On the other hand if diffusion (i.e. the parabolic character) dominates, practically any boundary condition can be imposed at any boundary. The situation is generalised to systems of equations by introducing the so called characteristic curves and surfaces.
Within the range of conditions allowed by the type of system of equations, the choice for each unknown at each particular boundary must be dictated by physics considerations.
The choice of the boundary conditions normally used in EDGE2D/U aims to simulate as closely as possible the physics constraints and in particular the external operational 'knobs' determining the plasma state in the region considered.

Boundary conditions for the temperature equations

The most important external parameters determining the electron and ion temperatures in the external region are the power P_e and P_i entering from the inner plasma (Fig. 1). This implies that a natural condition at this boundary is the energy flux for electrons and ions, normalised to prescribed values of P_e and P_i.
The values of P_e and P_i as well as the spatial distribution of the energy fluxes depend on the injected power (free external 'knob') but also on transport in the inner plasma. Standard choices, in line with our present understanding of transport in the inner plasma, are $P_e \approx P_i$ and a uniform energy flux distribution along the boundary, but these inputs to the code can be prescribed arbitrarily.
Alternatively it is possible to prescribe the ion and electron temperatures. This is however less satisfactory, from a predictive point of view, because these temperatures are indeed the result of transport and radiation losses in the region for a given input power.
It seems natural to impose zero heat flux ($\Rightarrow \partial T/\partial \rho = 0$) across the last flux surface towards any material wall (Fig. 1). However, this is realistic only as long as the computational region beyond the separatrix is much wider than typical temperature decay lengths in the SOL. Unfortunately this is not always the case in practice and a more general condition in the code allows to impose an exponential temperature decay at these boundaries.
The boundary conditions towards the targets are the simplest possible derived from sheath theory. For the electrons one has:

$$\frac{5}{2} n_e v_e T_e - \frac{h_\theta}{H_\theta} k_{\|}^e \frac{\partial T_e}{\partial \theta} = \beta_e n_e v_e T_e$$

and similarly for the ions.
The heat transmission coefficients β_e and β_i are normally assumed to be numbers, $\beta_e \approx 4.5$, $\beta_i \approx 2.5$. Other choices, based on sophisticated models of the transition from fluid to kinetic approximation in the proximity of the targets are available in the literature. However the

effective gain in accuracy remains a subject of debate, while they are rather cumbersome to deal with numerically. For this reason they have not been considered in EDGE2D/U so far.

Boundary conditions for the parallel momentum equations

The same considerations apply to the boundary conditions of the momentum equations at the targets. Complex models of the momentum transmission in the transition from a fluid to a kinetic approximation are available, but the standard choice remains $v_\alpha=c_s$, where c_s is the plasma sound speed. This is a restricted and not completely justified version of the condition $v\geq c_s$ first derived by Bohm for a plasma in contact with a metallic wall.
We remark that for an ion species like hydrogen, completely or almost completely recycled at the targets, the distribution of sources is strongly coupled to the velocity of the ion fluid at the targets. In fact a condition on the ion velocity determines the flow of entering neutrals and the density at the targets, and drives the plasma flux in the absence of pumping and puffing of neutrals.
In principle a supersonic flow in proximity of the targets can be driven by the conditions 'upstream'. For example this can be obtained in EDGE2D/U by imposing and maintaining a neutral influx at the targets corresponding to a supersonic ion velocity at the targets. In this case the imposed influx of neutrals drives the flow.
The presence of viscosity and convection of parallel momentum in the perpendicular direction requires boundary conditions for the parallel velocity v_α at the boundaries towards the inner plasma and the walls. In EDGE2D/U a value of v_α is prescribed at the interface with the inner plasma (usually $v_\alpha = 0$, but other values can be prescribed), while $\partial v_\alpha/\partial \rho = 0$ is assumed towards material walls.
It would be more satisfactory to prescribe the parallel momentum influx from the inner plasma, but no sufficiently reliable model of momentum deposition and transport in the inner plasma, e.g. from neutral beam injection, is presently available.

Boundary conditions for the density equations and schemes of neutral circulation

We discuss first the case of the hydrogenic ion density n_i. The external factors determining the distribution of n_i are refuelling via neutrals from target and walls and the influx Γ_i of ions from the inner plasma. The latter corresponds to deep refuelling by pellets or neutral beams and to neutrals leaving the external region and being ionised in the inner plasma.
As already observed the flux of neutrals from targets and walls in strongly correlated to the plasma outflux via recycling, but a least a fraction of it can be controlled by puffing and pumping. Deep refuelling is controllable.

Taking this into account the natural boundary conditions to be chosen in perpendicular direction are, similarly to the case of the temperature equations, the plasma influx from the inner plasma and zero outflux or an exponential decay of density toward the walls.
As long as a parallel ion flow towards the targets exists, the density at the target is determined by the flux and no boundary condition should be prescribed here.
Starting from an initial guess for the solution, a net influx of neutrals is given (usally but not necessarily from the targets) until a prescribed inventory N of ions in the region is obtained. In steady state N is kept constant by balancing any net outflux of ions with an equal influx of neutrals. The simulation of the time evolution from a steady state (i.e. from a proper initial condition) in response to fuelling variations is also possible by this method.
As an alternative the density at the inner plasma interface can be prescribed. However this is a computationally less efficient way to look for steady state solutions and does not allow to simulate realistically the effects of variations in the refuelling scheme.
The code can simulate various schemes of particle circulation. Ions leaving the region can either be completely recycled locally as neutrals or be partially recycled and partially absorbed. The absorbed fraction can reenter the region either as neutrals from a different boundary (gas puffing) or as ions from the inner plasma (deep fuelling). Similarly neutrals can either be totally reflected at boundaries or be partially absorbed and reinjected elsewhere. This technique has been applied to study the performance of the JET pumped divertor.
Recycling impurities such as neon are treated in the same way as hydrogenic ions. They are puffed as neutrals into the region from a chosen section of the wall boundary until a prescribed content is reached. Normally it is assumed that a steady state (i.e. zero flux) condition applies at the inner plasma interface for each impurity stage.
The treatment of intrinsic (non recycling) impurities such as carbon and beryllium is similar. These impurities are absorbed at targets and walls and are generated via sputtering by hydrogenic ions and neutrals, and by self sputtering. Injection of non recycling impurities is also possible.
The models used to simulate the interaction of atoms and ions with material walls (recycling, sputtering, etc.) are described in [4] and have been recently updated following [10].

Numerical Methods

Discretisation

The fluid equations are discretised on a non uniform grid defining n_α, T_e, T_i at cell centres whereas the parallel velocities v_α are defined at cell interfaces. The mesh follows contours in the magnetic coordinate ρ, but may not follow contours in the orthogonal poloidal coordinate θ allowing the mesh to be non orthogonal, e.g. in proximity of targets that are non orthogonal to poloidal magnetic field lines.

Flux divergence components in the θ direction are discretised using the usual three point scheme, with an upwind scheme to stabilise convective terms. For example, in the case of particle advection $\Gamma^{\theta} = n\,u$, where $u = \frac{Hh_{\theta}}{H_{\theta}} v_{\parallel}$

$$\frac{\partial(nu)}{\partial\theta} \Rightarrow \frac{\partial(nu)}{\partial\theta} - \frac{\partial}{\partial\theta}\left(\sigma\frac{\partial n}{\partial\theta}\right) \text{ with } \sigma = \frac{|u|}{2}\Delta\theta$$

In general a radial flux, Γ_{ρ}, has the form

$$\Gamma_{\rho} = \alpha\frac{\partial f}{\partial\rho} + \beta$$

The following procedure is adopted for the discretisation of the ρ derivative in order that the finite difference analogue of the continuity equation remains flux conservative. Applying Green's theorem to any quadrilateral cell yields

$$\frac{\partial\Gamma_{\rho}}{\partial\rho} \approx \frac{1}{\Delta\rho\Delta\theta}\left[\Gamma^{\rho}{}_{N}\Delta\theta_{N} + \Gamma^{\rho}{}_{W}\Delta\theta_{W} + \Gamma^{\rho}{}_{S}\Delta\theta_{S} + \Gamma^{\rho}{}_{E}\Delta\theta_{E}\right]$$

The $\Gamma_{\rho i}\Delta\theta_i$, i = {N, W, S,E}, are the radial fluxes through the North, West, South and East cell boundaries respectively. The fluxes $\Gamma_{\rho i}$ at cell boundary centres are evaluated by using isoparametric transformation techniques, common in Finite Element methods.
The resulting scheme relates a node to the 8 adjacent ones and in orthogonal cells reduces to the standard 3 point formulation for all radial derivatives. After linearisation, the linear system to be solved reads:

$$\sum_{m=-1}^{m=1}\sum_{n=-1}^{n=1} \mathbf{A}_{i,j}^{m,n} \bullet \mathbf{u}_{i+m,j+n} = \mathbf{b}_{ij}$$

Each discretised fluid equation is relaxed in turn in cyclic order until convergence is achieved after a few (usually ≈ 5) iterations.

Treatment of sources

Neutrals in most of the regimes of interest for plasmas in the external region are best treated by means of a Monte Carlo technique. This is done by the NIMBUS package that evaluates the density, temperature and velocity profiles of the neutral species. These profiles are frozen in between Monte Carlo calls and the inventory is rescaled at each step with the total particle

recycling flux. An update of the neutral profiles is performed at pre-assigned times, or is decided by the rate of the variation of certain indicators such as particle and energy sources (usually, a few percent of the total). This approach, while losing some details of the neutral energy spectrum, has nevertheless the advantage that source terms, including rate coefficients when closed formulas are available, can then be linearised in the plasma parameters, which helps to avoid instabilities and negative thermodynamic quantities in the high recycling regime. Statistical noise is reduced by the use of correlated random numbers [11], which ensure that, near convergence, subsequent Monte Carlo calls yield very similar neutral profiles irrespective of the number of histories.

Impurity charge states in the continuity and momentum equations are strongly coupled via atomic processes taking place on a very short time scale. To avoid unnecessarily short time steps, a splitting technique is used.

The fluid equations can be formally written as

$$\frac{\partial \mathbf{u}}{\partial t} = \mathbf{T}(\mathbf{u})$$

where $\mathbf{u} = (n_i, \mathbf{n}_z, v_i, \mathbf{v}_z, T_i, T_e)$. The solution u^τ after time step τ is obtained by solving in succession

$$\frac{1}{2}\frac{\partial \mathbf{n}_z^{\tau/2}}{\partial t} = \mathbf{S}_Z\left(\mathbf{n}_z^{\tau/2}\right) \qquad 0 < t < \tau/2$$

$$\frac{1}{2}\frac{\partial \mathbf{n}_z^{\tau/2}\mathbf{v}_z^{\tau/2}}{\partial t} = \mathbf{F}_Z\left(\mathbf{n}_z^{\tau/2}\mathbf{v}_z^{\tau/2}\right) \qquad 0 < t < \tau/2$$

$$\frac{1}{2}\frac{\mathbf{u}^\tau - \mathbf{u}^{\tau/2}}{\tau/2} = \mathbf{T}\left(\mathbf{u}^\tau\right) - \mathbf{S}\left(\mathbf{u}^\tau\right) \qquad \tau/2 < t < \tau$$

where $\mathbf{S} = (0, \mathbf{S}_Z, \mathbf{F}_Z, 0)$ and $\mathbf{S}_Z$, $\mathbf{F}_Z$ are the particle and momentum sources due to impurity ionisation and recombination. The first two substeps are integrated analytically for all impurity charge states since they are homogeneous systems of ordinary linear differential equations, whereas the third substep is solved by relaxing each equation separately in turn and iterating.

Predictive modelling of detached divertor plasmas in JET

Power exhaust in the ITER divertor is an important problem to be solved for the design of this device. A solution based on plasma extinction was suggested by P.H. Rebut and M.L. Watkins [12].

Plasmas that practically extinguish (detached plasmas) in the divertor region have been observed in several Tokamaks, including JET. However, for extrapolations to ITER, plasma detachment must be properly understood theoretically.

As a step in this direction an extensive campaign of numerical simulations has been carried out at JET in order to study some basic problems related to plasma detachment. The results reported here refer to predictions for the gas box divertor proposed as part of the JET divertor programme (Fig. 1).

Experimental results in detached plasma regimes suggest that particle, total momentum and total energy flows are strongly reduced at the divertor targets with respect to the case of attached plasmas with comparable values of input power in the SOL and of density upstream. Conservation laws imply that such a reduction must be the result of volume loss mechanisms for momentum and energy and possibly of perpendicular transport towards the side walls.

Simulations carried out for the old (pre 1993) JET configuration as well as for the present one (Mk I) have shown that volume losses related to the hydrogenic species (charge exchange and radiation) are not very efficient in dissipating power and are unlikely to be sufficient to cause full detachment at relevant values of the power P entering the external plasma region ($P \geq 2.5$ MW in JET [13], [14]). On the other hand, the same simulations show that hydrogenic neutrals can, at sufficiently low plasma temperature and not too high density, dissipate the plasma parallel momentum, as suggested in [15]. These results have been at least qualitatively confirmed by experimental observations [16]. Quantitative comparisons are expected to be possible with data from the upgraded diagnostic systems that have become available with the present divertor configuration.

These results imply that a radiative divertor, where impurity radiation plays a major role in dissipating power, may be required to solve the power handling problem. This approach presents however various problems. In particular one must ensure that impurities do not contaminate too much the inner plasma region. In addition recyclable impurities such as neon or argon should be used to avoid impurity accumulation at targets and walls. We remark that the production of intrinsic impurities via sputtering would be minimised inside the divertor in an almost extinguished plasma. Thus these impurities can be neglected in first approximation.

A number of simulations taking into account consistently impurity transport and radiation have been carried out, considering neon puffed into a pure plasma from the walls.

The same transport model across field line has been assumed for neon and hydrogenic ions. Details of such model, as well as preliminary comparisons with experimental results can be found in [17].

Our results show that a strong reduction of the power flowing to the targets, as well as a pressure drop typical of "detached" plasmas can be obtained by means of neon injection. For example with a content of neon in the external region equal to 1.5% the content of deuterium, 5.6 MW are radiated by neon out of 10 MW entering the SOL. Taking into account losses due to hydrogen radiation (1.9 MW) and the power flowing to the walls (1.4 MW mainly in the

divertor region), the total power flowing to the targets is reduced to 1.1 MW. The pressure drops by more than a factor of ten from midplane to the targets (fig. 2). The corresponding contour plots of electron temperature (fig. 3) shows a large region at low temperature (≤ 5 eV) in the divertor.

These results have been obtained with a realistic value of the density at the separatrix at mid plane, $n_s \approx 2 \times 10^{19}$ m^{-3}.

Unfortunately neon tends to reside and radiate mainly outside the divertor region (fig. 4a). We found that this result does not depend on where neon is puffed: puffing neon into the divertor does not change the result with respect to puffing it uniformly from the entire chamber wall. This is of course a dangerous situation because the impurities can diffuse from the SOL to the main plasma region. The situation might be improved by forcing a plasma flow towards the targets so that the friction force of deuterium on impurities overcomes the thermal force that drives the impurities away from the divertor [6].

Such a forced flow can be achieved by pumping neutrals in the divertor and by injecting them upstream. In our computations pumping has been simulated by albedo coefficients, (A in Fig. 2), evaluated by means of the Monte Carlo neutral code EIRENE [18] and should therefore not be unrealistic [19].

The effect of the induced flow on the neon distribution for the case discussed so far is strong as illustrated in Fig. 4b. The radiated power is somewhat reduced (4 MW) but the power flowing to the targets remains low (2 MW). One might expect that with a divertor region more extended in the poloidal direction, the retention of neon in the divertor would improve even further. This is confirmed by simulations carried out for ITER [20].

These simulations indicate that a divertor relying upon dissipation of power by means of radiation of a recyclable impurity such as neon might work in practice. Clearly the problem of power handling and impurity control become strictly linked in this concept and the divertor must be optimised having this in mind. For example an important question not addressed so far is the optimisation of the divertor configuration in terms of the possibility of inducing a beneficial plasma flow.

Obviously one cannot think to solve the problems connected with the radiative divertor concept only by means of predictive simulations such as those presented here. Much more theoretical work and extensive analysis of experimental data are required in order to obtain a better understanding of transport, and in particular impurity transport, in the plasma boundary region. However it is expected that codes such as EDGE2/U and NIMBUS, improved and better validated against experimental results, will continue to play an important role in the solutions of these, and other important problems.

Acknowledgements

We are indebted to K.E. Borrass, L.D. Horton, A. Loarte, G.F. Matthews and G.C. Vlases for useful discussions.

References

[1] Ueda, N., et al., Contributions to Plasma Physics, 34 (1994) 350.

[2] Reiter, D., Journal of Nuclear Materials, 196-198 (1992) 80.

[3] Taroni, A., et al., Contributions to Plasma Physics, 32 (1992) 438.

[4] Cupini, E., De Matteis, A., Simonini, R., The Monte Carlo code NIMBUS, NET Report EUR XII - 324/9 (1984).

[5] Summers, H.P., von Hellermann, M., Atomic and Molecular Data Exploitation for Spectroscopic Diagnostic of Fusion Plasmas, Report JET-P(93) 35.

[6] Keilhacker, M., et al., Nuclear Fusion, 31 (1991) 535.

[7] Igitkhanov, Yu. L., Contributions to Plasma Physics, 28 (1988) 477.

[8] Radford, G., Contributions to Plasma Physics, 32 (1992) 297.

[9] Janev, R.K., et al. Elementary Processes in Hydrogen-Helium Plasmas, Springer Verlag (1987).

[10] Eckstein, W., et al., Max Planck Institute for Plasma Physics Report, IPP 9/82 (1993).

[11] Cenacchi, G. and De Matteis, A., Num. Math. 16 (1970) 11.

[12] Watkins, M.L. and Rebut, P.H., 19th Europ. Conf. on Contr. Fusion and Plasma Phys., Innsbruck, Austria (1992).

[13] Taroni, A., et al., 11th Int. Conf. on Plasma Surface Interactions in Controlled Fusion Devices, Mito, Japan (1994), to appear in Journal of Nuclear Materials.

[14] Simonini, R., et al., 21st Europ. Conf. on Contr. Fusion and Plasma Phys., Montpellier, France (1994).

[15] Borrass, K. and Stangeby, P., 20th Europ. Conf. on Contr. Fusion and Plasma Phys., Lisbon (1993).

[16] Horton, L.D., et al., 21st Europ. Conf. on Contr. Fusion and Plasma Phys., Montpellier, France (1994).

[17] Loarte, A., et al., 11th Int. Conf. on Plasma Surface Interactions in Controlled Fusion Devices, Mito, Japan, (1994), to appear in Journal of Nuclear Materials.

[18] Reiter, D., The EIRENE code, version Jan. 92, Technical Report Jül-2599, KFA Jülich, Germany, 1992.

[19] Deksnis, E.B., Private communication.

[20] Weber, S.A., et al., This workshop.

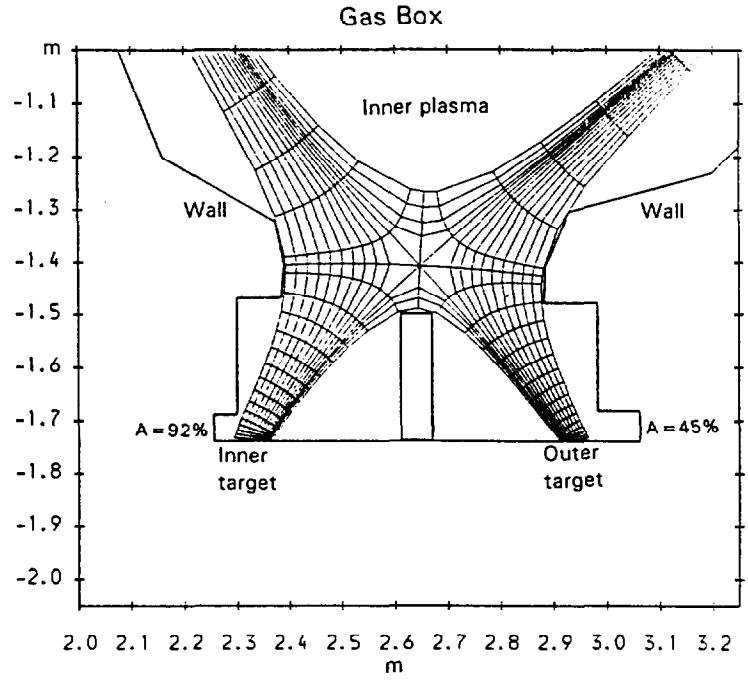

Fig. 1 JET gas box divertor configuration, with computational mesh and albedo values for neutrals (A) at the entrance of the pumping ducts.

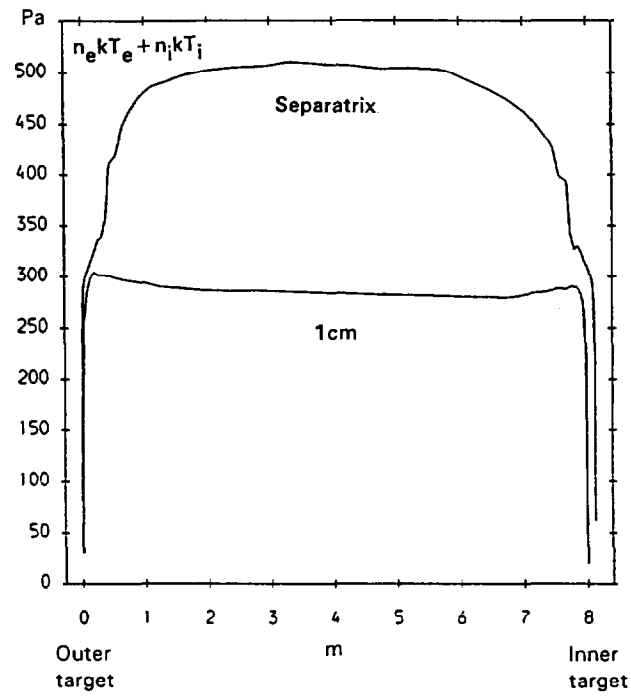

Fig. 2 Plasma pressure along separatrix and along magnetic field line 1 cm outside separatrix.

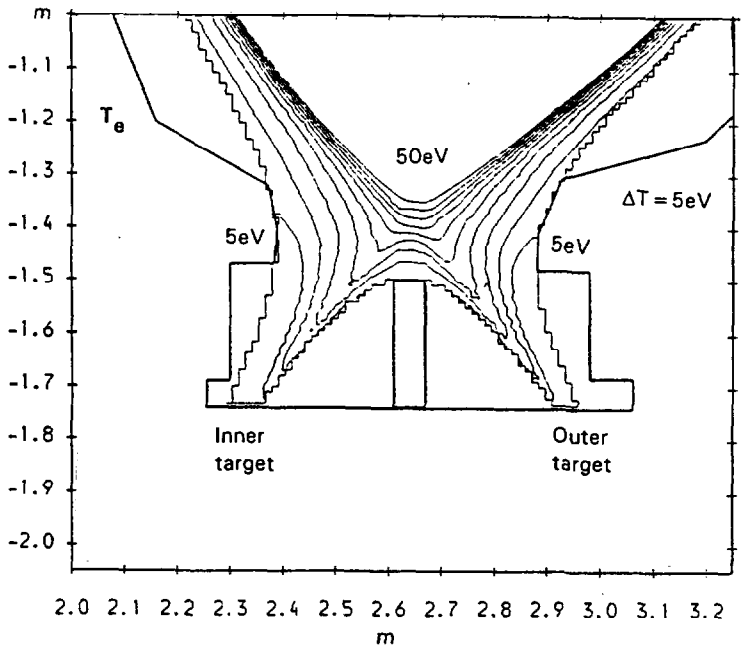

Fig. 3 Contour plot of T_e.

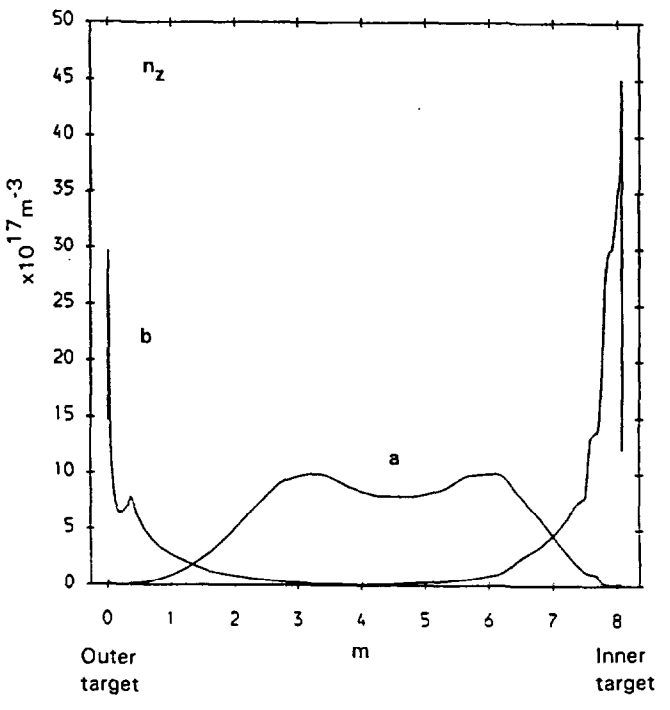

Fig. 4 Impurity density n_z averaged across the SOL as a function of distance along separatrix in the poloidal plane.